# Identification and control of stick-slip vibrations using Kalman estimator in oil-well drill strings

Liu Hong, Irving P. Girsang and Jaspreet S. Dhupia

School of Mechanical and Aerospace Engineering, Nanyang Technological University
50 Nanyang Avenue, Singapore 639798
Email: hong0126@e.ntu.edu.sg, irving1@e.ntu.edu.sg, djaspreet@ntu.edu.sg

## Abstract

Excessive stick-slip vibrations of drill strings can cause premature component failures and inefficient drilling operations. Previous research works employ real-time measurements of all states of the drill string as feedback to the controllers to suppress such vibrations. While real-time measurements are readily available for components at the surface, only limited measurements are practically available for the downhole states. To address the requirement for downhole states, this paper proposes the utilization of Kalman estimator to estimate the downhole drill bit position and velocity based on the measurements at the surface. In the design of the estimator, the nonlinear downhole friction torque is approximated by a linear persistent disturbance model. A linear-quadratic-Gaussian (LQG) control strategy is then applied on the estimated states to mitigate the unwanted vibrations. Performance of this control scheme is investigated through numerical simulations where the dynamics of the drill string is modeled using a high fidelity lumped parameter model considering torsional stick-slip and lateral motions as well as a nonlinear friction model. The dynamic response from the high fidelity model is demonstrated to have a close qualitative agreement with the stick-slip vibrations observed in field. The simulated results demonstrate the capability of the proposed Kalman estimator in identifying the stick-slip vibrations and estimating the downhole friction torque. The effectiveness of the proposed controller in avoiding such vibrations is also verified.

## 1. Introduction

Deep wells for oil and gas production are drilled using a drill string to create boreholes. The main components of an industrial oil-well drill string are the top rotary mechanism

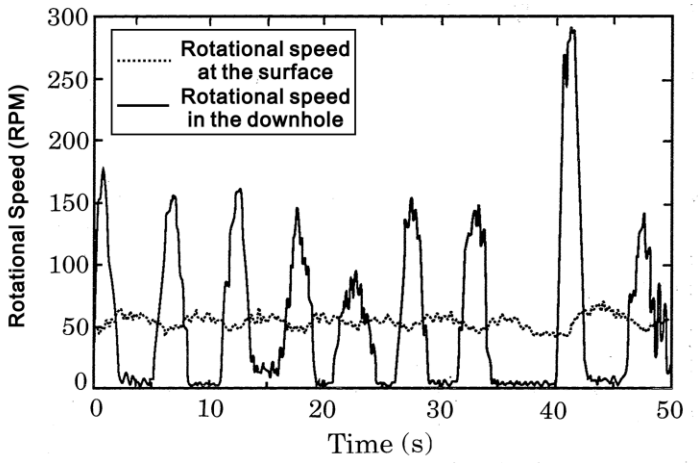


Fig.1. Field observed stick-slip vibration (reproduced from Jansen and Steen, 1995).

(rotary table or top drive), drill pipes and bottom hole assembly (BHA). To turn the drill bit, the entire drill string is rotated at the surface using the top rotary mechanism. The segmented drill pipes are joined together to connect the top rotary mechanism with the BHA. The dynamics of drill strings has complex characteristics such as coupled axial, lateral and torsional vibrations as well as hysteretic downhole friction (Jansen and Steen, 1995, Leine et al., 2002). The nonlinear friction, which is characterized by a high friction torque at low drill bit speed but lower torques at higher drill bit speed, can excite stick-slip vibrations (Tjahjowidodo, 2012). Such stick-slip vibrations occur in drilling deep wells when the BHA is momentarily caught by the bit-rock interaction friction torque (i.e., stick) and then suddenly released (i.e., slip). The sudden release of stored potential energy in the flexible drill strings during the slip phase can vary the rotational speed of the BHA from zero to as much as six times the speed of the top rotary mechanism, which is typically controlled at constant reference (Jansen and Steen, 1995). Figure 1 illustrates an example of stick-slip vibration from field measurement. Typical period of such vibrations ranges from 2 to 15 seconds (National Oilwell Varco, 2012). Further, the severe torsional vibrations in drill strings result in large centrifugal accelerations that excite the coupled lateral vibrations, which can make the drill string hit the borehole wall (Yigit and Christoforou, 1998). These undesired torsional and lateral vibrations result in excessive bit wear, premature tool failures and poor drilling rates.

Active controls are required to prevent the occurrence of such undesired vibrations. Various state-space based control designs, such as optimal control and sliding mode

control, have been proposed to mitigate the stick-slip vibrations of drill strings (Al-Hiddabi et al., 2003, Zamanian et al., 2007, Richard et al., 2007, Ritto et al., 2009 and Yigit and Christoforou, 2002). However, they usually require real-time downhole state measurements whereas most of the current industrial monitoring systems only provide real-time measurements at the surface of the well (such as the rotational speed of the top rotary mechanism or the input torque from the motors at the surface) (National Oilwell Varco, 2012).

To address the lack of downhole information, this paper employs a Kalman estimator to estimate the downhole states and the downhole friction torque based on measurements at the top rotary mechanism. The estimation of the downhole friction torque, which is hysteretic in nature, is enabled by adopting a linear persistent disturbance model. Based on the state estimates, a linear-quadratic regulator (LQR) is designed to suppress the undesired vibrations while maintaining desired speeds of the downhole and top rotary mechanism. For efficient implementation, the estimator and controller are designed based on a simple purely torsional two degrees of freedom (DOFs) lumped parameter model.

To assess the controller performance under realistic conditions, a high fidelity lumped parameter model of the drill string is developed in this paper to simulate the characteristic stick-slip vibrations of the drill string. The model is extended from the purely torsional lumped parameter models of the drill strings (Jansen, 1991, Puebla and Ramirez, 2008 and Lope and Cortes, 2007a) to include both torsional and lateral DOFs of the drill collars. The downhole friction is represented using a hysteretic dry friction formulation with Stribeck curve. The dynamic response obtained from this presented model is shown to have a close qualitative agreement with the field observations in terms of stick-slip vibrations. Hence, the extended model can represent the true plant for validation of controllers.

The rest of the paper is organized as follows. In Section II, the coupled torsional and lateral vibration model and the hysteretic dry friction model are described. The proposed LQG control strategy to suppress the undesired drill string vibrations is presented in Section III. Section IV discusses the simulated performance of the designed Kalman

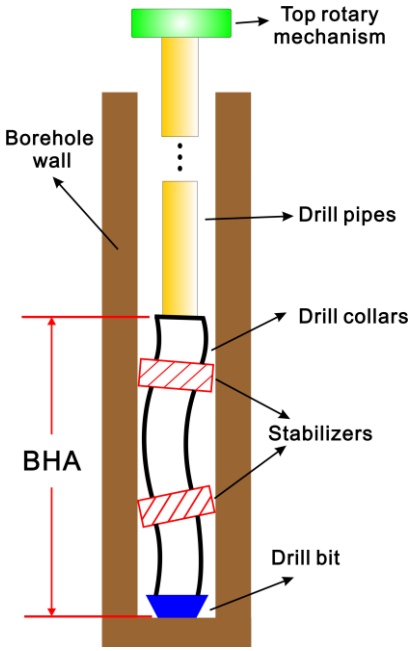


Fig.2. Typical schematic of a drill string.

estimator and LQR in terms of mitigating torsional and lateral vibrations. Finally, Section V concludes the paper.

## 2. Dynamic model of drill strings

Figure 2 illustrates the typical scheme of a drill string used for making borehole for oil wells. In this work, it is assumed that the well is vertical and drill string is straight and initially centred without any bending or inclination angle. The drill string partly rests on the bit such that a compressive force of $10^4$ to $10^6$ N is applied on the bit to aid in penetration (Lopez and Cortes, 2007b) while maintaining the drill pipes in tension to avoid buckling. This compressive force on drill collars is referred as the weight on bit (WOB). The long and thin drill pipes result in a torsional rigidity that is much lower than that of the drill collars. Besides torsional vibrations, these drill collars also experience lateral vibrations due to the compressive force and their own eccentricity. Excessive lateral vibrations can cause impacts between the drill collars and borehole wall, as often observed in field measurements (Tucker and Wang, 1999; Hong and Dhupia, 2015).

While finite element modeling approach can be used to simulate responses of drill strings, it is computationally heavy and time consuming to solve them. Therefore, it is

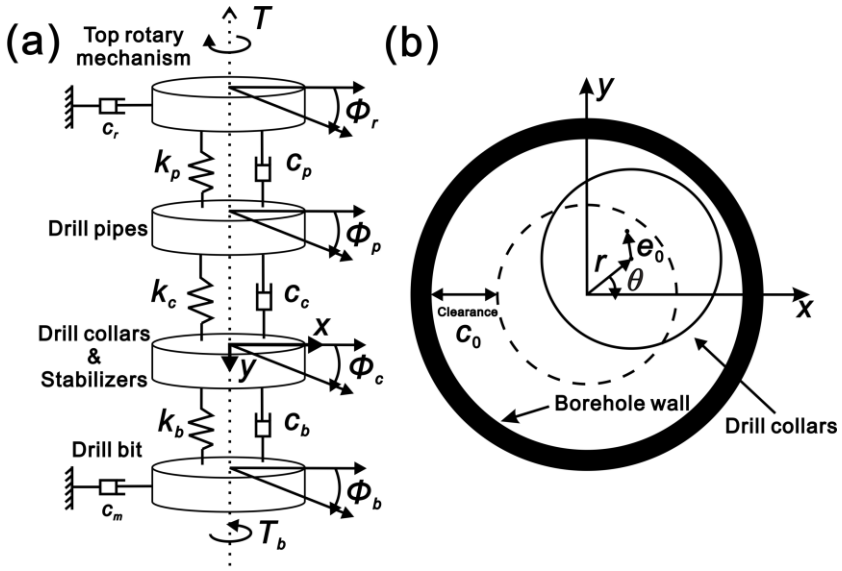


Fig.3. (a) Lumped parameter model of a drill string; (b) Cross-section view of the lateral motion of the drill collars and stabilizers.

necessary to develop high fidelity torsional lumped parameter models which are more efficient to study the dynamics of drill strings especially for real-time implementation (Jansen, 1991, Puebla and Ramirez, 2008 and Lopez and Cortes, 2007a). The models are also often treated as the true plant (Girsang et al., 2014) to verify control performance for drill strings applications (Al-Hiddabi et al., 2003, Zamanian et al., 2007, Richard et al., 2007, Ritto et al., 2009 and Yigit and Christoforou, 2002). In this paper, a lumped parameter model shown in Fig. 3 is used to represent the drill string assembly. Compared with the existing purely torsional models in literatures, the proposed model takes into account the lateral motion of the drill collars on the indicated *x*-*y* plane, which is critical to describe the impacts between the drill collars and borehole wall. The top rotary mechanism, drill pipes, drill collars and drill bit are respectively lumped as rotational inertias *J* connected to each other through linear torsional springs and dampers as depicted in Fig. 3(a). The lateral motion is represented using a polar coordinate attached to the borehole center as shown in Fig. 3(b). The DOFs of the lumped parameter model are defined in vector **Q** as

$$\mathbf{Q} = \left[\phi_r, \phi_p, \phi_c, r, \theta, \phi_b\right]^T \tag{1}$$

where $\phi$ represents the angular displacement of the subscripts *r*, *p*, *c* and *b* corresponding to the top rotary mechanism, drill pipes, drill collars and drill bit, respectively, while *r* and $\theta$ represent the lateral displacement of the drill collars. From Newton's second law, the equations of motion of the drill string can be expressed as

$$J_r\ddot{\phi}_r = T - c_r\dot{\phi}_r - k_p\left(\phi_r - \phi_p\right) - c_p\left(\dot{\phi}_r - \dot{\phi}_p\right) \tag{2}$$

$$J_p\ddot{\phi}_p = k_p\left(\phi_r - \phi_p\right) + c_p\left(\dot{\phi}_r - \dot{\phi}_p\right) - k_c\left(\phi_p - \phi_c\right) - c_c\left(\dot{\phi}_p - \dot{\phi}_c\right) \tag{3}$$

$$\begin{aligned} J_c\ddot{\phi}_c = {} & k_c\left(\phi_p - \phi_c\right) + c_c\left(\dot{\phi}_p - \dot{\phi}_c\right) - k_b\left(\phi_c - \phi_b\right) - c_b\left(\dot{\phi}_c - \dot{\phi}_b\right) \\ & + F_r e_0 \sin\left(\phi_c - \theta\right) + F_\theta\left(R - e_0\cos\left(\phi_c - \theta\right)\right) \\ & - c|v|e_0\left(\dot{r}\sin\left(\phi_c - \theta\right) + r\dot{\theta}\cos\left(\phi_c - \theta\right)\right) \end{aligned} \tag{4}$$

$$m\left(\ddot{r} - r\dot{\theta}^2\right) = me_0\left(\dot{\phi}^2\cos\left(\phi_c - \theta\right) + \ddot{\phi}\sin\left(\phi_c - \theta\right)\right) + F_r - kr - c|v|\dot{r} \tag{5}$$

$$m\left(r\ddot{\theta} + 2\dot{r}\dot{\theta}\right) = me_0\left(\dot{\phi}^2\sin\left(\phi_c - \theta\right) - \ddot{\phi}\cos\left(\phi_c - \theta\right)\right) + F_\theta - c|v|r\dot{\theta} \tag{6}$$

$$J_b\ddot{\phi}_b = k_b\left(\phi_c - \phi_b\right) + c_b\left(\dot{\phi}_c - \dot{\phi}_b\right) - c_m\dot{\phi}_b - T_b\left(\dot{\phi}_b, \ddot{\phi}_b\right) \tag{7}$$

where *T* is the input torque from the motor driving the top rotary mechanism, $k_i$ and $c_i$ are respectively the effective torsional stiffness and damping of each component represented by the subscript $i \in \{r, p, c, b, m\}$ in Fig. 3(a) where the subscript *m* corresponds to the mud. *R* is the radius of the drill collars. $e_0$ is the eccentricity of the center of mass with respect to the geometric center of the collar section, $v = r\dot{\theta} + R\dot{\phi}_c$ is the relative linear velocity between the borehole wall and the drill collar, *m*, *k* and *c* are the effective mass of the drill collars with the fluid mud, bending stiffness and bending damping of the collars, respectively. The contact force $F_r$ between the drill collars and borehole wall is modeled by a formulation similar to that of a linear spring with pre-defined clearance $c_0 = R_h - R$ as (Jansen, 1993)

$$F_r = \begin{cases} -k_w\left(r - c_0\right) - c_w\dot{r}, & r \geq c_0 \\ 0, & r < c_0 \end{cases} \tag{8}$$

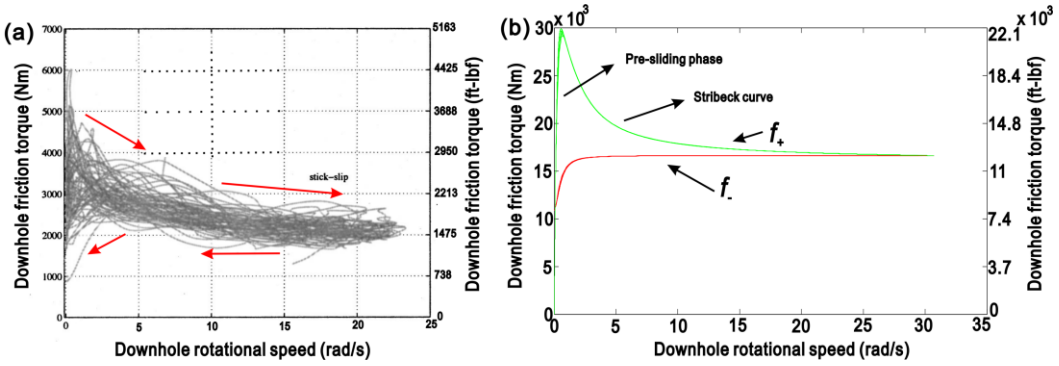


Fig.4. (a) Measurements of the downhole hysteretic friction from a full scale research rig (reproduced from Leine et al., 2002); (b) Hysteretic dry friction model presented in Eqs. (10) – (14).

$$F_\theta = -\mu_w \mathrm{sgn}(v) F_r \tag{9}$$

where $R_h$ is the radius of the borehole wall, $k_w$ and $c_w$ are respectively the stiffness and damping coefficients of the borehole wall, and $\mu_w$ is the friction coefficient between the drill collars and the borehole wall.

A measured friction curve of the BHA of a research rig during stick-slip vibrations, which relates the downhole friction torque to the downhole rotational speed, is shown in Fig. 4(a). This experimentally measured downhole friction torque exhibits a hysteretic behavior and negative Stribeck curve with respect to the bit rotational speed. Thus, the downhole friction torque $T_f$ can be approximated using a hysteretic dry friction model as (Yigit and Christoforou, 2002 and Wojewoda et al., 2008)

$$T_f\left(\dot{\phi}_b, \ddot{\phi}_b\right) = \begin{cases} W_{ob} R f_+\left(\dot{\phi}_b\right), & \mathrm{sgn}(\dot{\phi}_b \ddot{\phi}_b) > 0 \\ W_{ob} R f_-\left(\dot{\phi}_b, \ddot{\phi}_b\right) \mathrm{sgn}\left(\dot{\phi}_b\right), & \mathrm{sgn}\left(\dot{\phi}_b \ddot{\phi}_b\right) < 0 \end{cases} \tag{10}$$

where

$$f_+\left(\dot{\phi}_b\right) = \tanh\left(\dot{\phi}_b\right) + \frac{\alpha_1 \dot{\phi}_b}{\left(1 + \alpha_2 \dot{\phi}_b^{\,2}\right)} \tag{11}$$

$$f_-\left(\dot{\phi}_b, \ddot{\phi}_b\right) = \left(0.97 - \frac{f_1\left(\dot{\phi}_b\right) - f_2}{f_2} g\left(\dot{\phi}_b, \ddot{\phi}_b\right)\right) \tag{12}$$

$$f_1\left(\dot{\phi}_b\right) = f + \Delta f \frac{1}{1+\left|\frac{\dot{\phi}_b}{v}\right|} \tag{13}$$

$$g\left(\dot{\phi}_b, \ddot{\phi}_b\right) = \frac{1}{1+\left(\frac{\dot{\phi}_b - \tau\ddot{\phi}_b}{v}\right)^2} \tag{14}$$

The hysteretic model formulated in (10) is depicted in Fig. 4(b). Equation (11) describes the pre-sliding and acceleration phase with $\alpha_1 = 7$ and $\alpha_2 = 6$ to model the Stribeck curve. Equations (12) – (14) represent the deceleration phase in which the constants are $f_2 = 0.25$, $f = 0.32$, $\Delta f = 0.02$, $v = 0.6$ and $\tau = 0.002$. It is noteworthy that Fig. 4 presents only the positive rotational speed because in drilling application a negative rotational speed (i.e., speed in the reverse direction) cannot be applied as it will uncoil the drill pipes.

The bit-rock interaction torque $T_b$ in (7) can be expressed as

$$T_b = \begin{cases} T_d, & \text{if } \left|\dot{\phi}_b\right| < D_v \text{ and } T_f \geq \left|T_d\right| \\ T_f, & \text{else} \end{cases} \tag{15}$$

where $D_v = 10^{-3}$ is chosen as a small positive constant to denote the zero velocity band and the function $T_d$ represents the effective driving torque acting on the drill bit transmitted through the torsional spring and dampers by

$$T_d\left(\phi_c, \phi_b, \dot{\phi}_c, \dot{\phi}_b\right) = k_c\left(\phi_c - \phi_b\right) + c_c\left(\dot{\phi}_c - \dot{\phi}_b\right) - c_b\dot{\phi}_b \tag{16}$$

## 3. Kalman estimator and LQR design

As discussed in the previous sections, the downhole measurements are required by industrial systems to identify the occurrence of stick-slip vibrations. These measurements are also required by the state-space based controller designs in previously reported research works (Al-Hiddabi et al., 2003, Zamanian et al., 2007, Richard et al., 2007, Ritto et al., 2009 and Yigit and Christoforou, 2002). However, in practice, measurements are usually only available from the components at the surface. Thus, this paper employs an LQG control technique to observe the occurrence of stick-slip

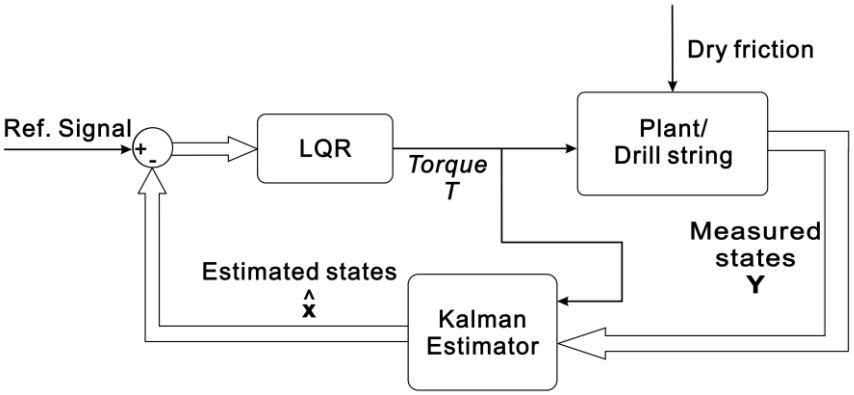


Fig.5. Schematic of the proposed feedback closed loop control strategy.

vibrations without any downhole measurements and avoid the vibrations while regulating the speed of the drill string at a given constant reference speed $v_{ref}$. This proposed technique, whose schematic is shown in Fig. 5, employs a Kalman estimator to estimate the states of the downhole drill bit. An optimal LQR control law is then later formulated to mitigate the undesired vibrations based on the estimated states.

To achieve efficient implementation, the estimator and controller designs are based on a reduced order two DOFs model of the drill strings shown in Fig. 6 and represent by following set of equations

$$J_1\ddot{\phi}_r + k_T\left(\phi_r - \phi_b\right) + c_T\left(\dot{\phi}_r - \dot{\phi}_b\right) = T \tag{17}$$

$$J_2\ddot{\phi}_b - k_T\left(\phi_r - \phi_b\right) - c_T\left(\dot{\phi}_r - \dot{\phi}_b\right) = -T_{opp} \tag{18}$$

where, $J_1 = J_r + J_p$ and $\phi_r$ denote the equivalent inertia of the top rotary mechanism and drill pipes and angular displacement of the components available at the surface; while $J_2$

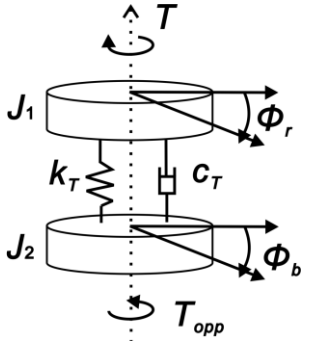


Fig.6. Pure torsional reduced order drill string model.

= $J_c$ + $J_b$ and $\phi_b$ denote the equivalent inertia and angular displacement of the BHA in the downhole. $k_T$ and $c_T$ respectively represent the equivalent torsional stiffness and damping respectively, evaluated as $\frac{1}{k_T}=\frac{1}{k_p}+\frac{1}{k_c}+\frac{1}{k_b}$ and $c_T=0.08\times k_T$. The lateral motion is not included in this reduced order purely torsional model. It is noteworthy the resulting controller is later applied on the high fidelity model developed in Eqs. (2) – (7), which is assumed as the true plant model to evaluate its performance.

The state-space representation of the reduced order model can be written as

$$\dot{\mathbf{x}}=\mathbf{A}_m\mathbf{x}+\mathbf{B}_m T+\mathbf{B}_{d,m}T_{opp} \tag{19}$$

where the **x** is the state vector defined as:

$$\mathbf{x}=\left[\phi_r,\phi_b,\dot{\phi}_r,\dot{\phi}_b\right]^T \tag{20}$$

$\mathbf{A}_m$ is the state matrix, while $\mathbf{B}_{m,}$ and $\mathbf{B}_{d,m}$ are the controlled input and disturbance input matrices

$$\mathbf{A}_m=\begin{bmatrix} 0 & 0 & 1 & 0 \\ 0 & 0 & 0 & 1 \\ \frac{-k_T}{J_1} & \frac{k_T}{J_1} & \frac{-c_T}{J_1} & \frac{c_T}{J_1} \\ \frac{k_T}{J_2} & \frac{-k_T}{J_2} & \frac{c_T}{J_2} & \frac{-c_T}{J_2} \end{bmatrix} \tag{21}$$

$$\mathbf{B}_m=\begin{bmatrix} 0 & 0 & \frac{1}{J_1} & 0 \end{bmatrix}^T \tag{22}$$

$$\mathbf{B}_{d,m}=\begin{bmatrix} 0 & 0 & 0 & -\frac{1}{J_2} \end{bmatrix}^T \tag{23}$$

The opposing torque $T_{opp}$ is the linear estimate of the downhole friction $T_f$. It is assumed that $T_{opp}$ is a step persistent disturbance input whose dynamics is represented as (Girsang and Dhupia, 2013)

$$\begin{aligned} \dot{x}_{d,m} &= w \\ T_{opp} &= x_{d,m} \end{aligned} \tag{24}$$

where $x_{d,m}$ is the disturbance state and $w$ is a zero mean Gaussian white noise. Thus, the augmented state-space representation of the controlled plant model is

$$\begin{aligned} \dot{\mathbf{x}}_0 &= \mathbf{A}_0\mathbf{x}_0 + \mathbf{B}_0 T + \mathbf{D}_0 w \\ \begin{bmatrix} \dot{\mathbf{x}} \\ \dot{x}_{d,m} \end{bmatrix} &= \begin{bmatrix} \mathbf{A}_m & \mathbf{B}_{d,m} \\ \mathbf{0} & 0 \end{bmatrix} \begin{bmatrix} \mathbf{x} \\ x_{d,m} \end{bmatrix} + \begin{bmatrix} \mathbf{B}_m \\ 0 \end{bmatrix} T + \begin{bmatrix} \mathbf{0} \\ 1 \end{bmatrix} w \end{aligned} \tag{25}$$

The output equations can be written in terms of the augmented state vector $\mathbf{x}_0$, which contains the states for both the system and downhole friction torque disturbance.

$$\mathbf{y} = \begin{bmatrix} \phi_r & \dot{\phi}_r \end{bmatrix}^T = \mathbf{C}_0\mathbf{x}_0 \tag{26}$$

with $\mathbf{C}_0 = \begin{bmatrix} 1 & 0 & 0 & 0 & 0 \\ 0 & 0 & 1 & 0 & 0 \end{bmatrix}$ represents that only the states of the top rotary mechanism are measured. Here, ($\mathbf{A}_0$, $\mathbf{C}_0$) can be verified to be observable. Thus, even though the states of the drill bit and the disturbance state are not measured, an optimal estimator such as Kalman estimator, can be implemented to estimate the unmeasured plant and disturbance states by properly chosen the Kalman gain **L**. The estimator dynamics are then written as (George et al., 2008)

$$\dot{\hat{\mathbf{x}}}_0 = \mathbf{A}_0\hat{\mathbf{x}}_0 + \mathbf{B}_0 T + \mathbf{L}\left(\mathbf{y}_0 - \hat{\mathbf{y}}_0\right) \tag{27}$$

where the symbol ^ represent the estimated states and the Kalman gain matrix **L** can be calculated as $\mathbf{L} = \mathbf{P}\mathbf{C}^T{}_0\mathbf{R}^{-1}$. The estimation error covariance $\mathbf{P} = E\left[\left(\mathbf{x}_0 - \hat{\mathbf{x}}_0\right)\left(\mathbf{x}_0 - \hat{\mathbf{x}}_0\right)^T\right]$ is obtained by solving the continuous-time Riccati equation

$$\dot{\mathbf{P}} = \mathbf{A}_0\mathbf{P} + \mathbf{P}\mathbf{A}^T{}_0 - \mathbf{L}\mathbf{C}_0\mathbf{P} + \mathbf{D}_0 Q \mathbf{D}^T{}_0 \tag{28}$$

where $Q$ and **R** are the weighting factors.

($\mathbf{A}_m$, $\mathbf{B}_m$) can also be verified as controllable. Thus, an LQR can be designed to minimize the following cost function with the weighting factors $\mathbf{Q}_c$ and $R_c$,

$$C = \frac{1}{2}\int_0^{\infty}\left(\mathbf{x}^T\mathbf{Q}_c\mathbf{x} + R_c T^2\right)dt \tag{29}$$

The control goal is to suppress the stick-slip vibrations while maintaining a desired bit and top rotary mechanism speed, $\dot{\phi}_b$ and $\dot{\phi}_r$, with respect to the given constant reference speed $v_{ref}$. Thus, the control input is designed as

$$T = k_1\int_0^t\left(v_{\text{ref}} - \dot{\hat{\phi}}_r\right)d\tau + k_2\int_0^t\left(v_{\text{ref}} - \dot{\hat{\phi}}_b\right)d\tau + k_3\left(v_{\text{ref}} - \dot{\hat{\phi}}_r\right) + k_4\left(v_{\text{ref}} - \dot{\hat{\phi}}_b\right) \tag{30}$$

where the gain matrix $\mathbf{K} = \begin{bmatrix} k_1 & k_2 & k_3 & k_4 \end{bmatrix} = \frac{1}{R_c}\mathbf{B}_m^T\mathbf{P}_c$, solves the Riccati equation for the controller (Freudenberg et al., 2003)

$$\mathbf{A}_m^T\mathbf{P}_c + \mathbf{P}_c\mathbf{A}_m - \frac{1}{R_c}\mathbf{P}_c\mathbf{B}_m\mathbf{B}_m^T\mathbf{P}_c + \mathbf{Q}_c = \mathbf{0} \tag{31}$$

## 4. Simulations results

The simulations are implemented in the MATLAB/Simulink environment. The parameters of the drill string were chosen according to those of typical oil well drilling rig (Jansen and Steem, 1995, Lopez and Cortes, 2007a and National Oilwell Varco, 2012).

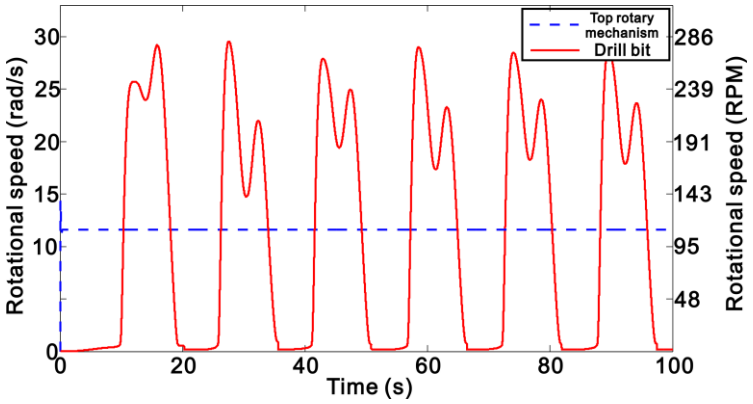


Fig.7. Simulated rotational speed of the top rotary mechanism at the surface and the drill bit in the downhole.

They are provided in the Appendix. The equations of motion, (2)-(16), are numerically solved, where the initial lateral displacement of the drill collars was assigned to be 0.03m (1.18in) and the clearance $c_0$ between the drill collars and the borehole wall was set as 0.1m (3.94in).

As a reference case, the common industrial PI control strategy was applied to regulate the speed of the top rotary mechanism at the surface. The classical PI controller, based on the error in the rotational speed of the top rotary mechanism, was tuned using the Ziegler-Nichols method (Lopez and Suarez, 2004) so that the top rotary mechanism follows a constant reference speed 11.6rad/s (110RPM), which is a typical nominal operating speed of oil well drilling systems (Leine et al., 2002 and Lopez and Cortes, 2007b). Figure 7 shows the simulated rotational speed of both the top rotary mechanism and downhole drill-bit. Even though the top rotary mechanism is controlled to operate at the constant

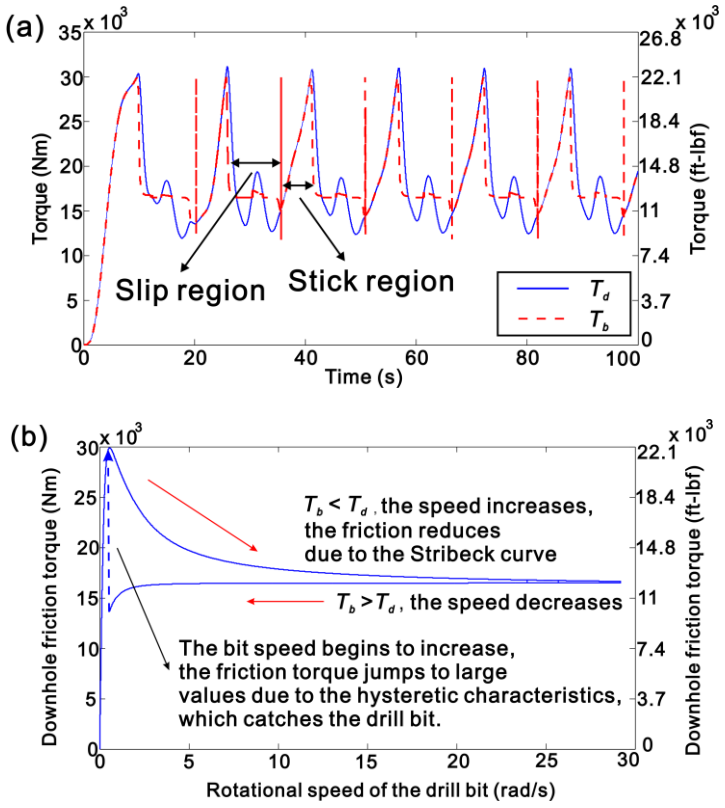


Fig.8. (a) Bit-rock interaction torque $T_b$ and driving torque $T_d$ transmitted through the torsional spring; (b) Typical downhole friction torque variation with respect to the downhole speed during a cycle of stick-slip vibration.

reference value, where there is an obvious torsional vibration at the drill bit. The drill bit response shows good qualitative agreement with stick-slip vibrations observed through field measurements (e.g., the one in Fig. 1) in terms of period and amplitude. Such torsional vibrations often occur in practice because the tuning of the PI controller does not take into the account of the drill bit speed, which is often unavailable for measurements. Therefore, although the speed of the top rotary mechanism is successfully regulated, the speed of the downhole drill bit fluctuates from 0 to 29 rad/s (nearly three times the speed at the surface) with a typical period of 15 seconds. This phenomenon can remain unnoticed unless the rotational speed of the bit is monitored. As illustrated in Fig. 8(a), when the bit is momentarily caught (i.e., when its rotational speed is nearly zero), the driving torque acting on the bit $T_d$ increases to a large value to overcome the static dry friction. However, when the bit is released, the friction torque decreases following the Stribeck curve during which the release of the energy stored in the drill strings results in large accelerations of the bit. The sudden increase in the bit speed reduces the deflection across the drill pipes, which in turn reduces the driving torque less than the friction torque causing the bit to decelerate. Under a sustained stick-slip vibration, the drill bit speed can drop down to nearly zero. Then, due to the hysteretic characteristic of the dry friction, the friction torque can suddenly increase to a large value catching the drill bit as shown in Fig. 8(b). When the driving torque is larger than the friction torque, the bit speed will increase, and the cycle repeats. The large amplitude of such torsional vibration can result in large centrifugal accelerations, which further excite excessive coupled lateral vibrations, as illustrated in Fig. 9.

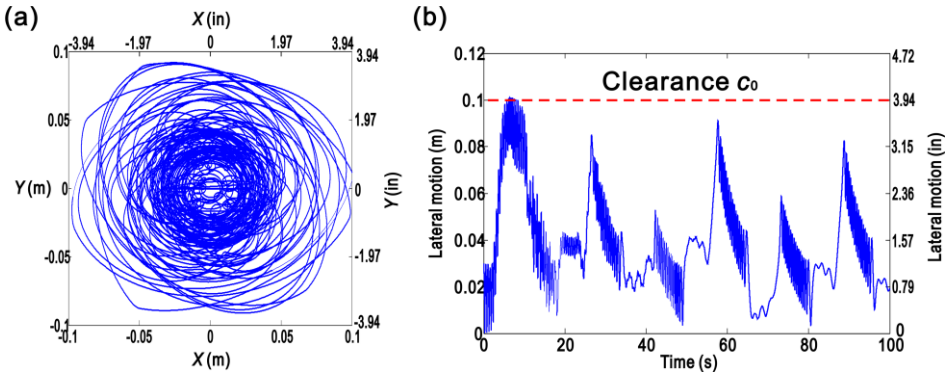


Fig.9. (a) Trajectory of the geometric center of the drill collars controlled by the common PI; (b) Lateral vibrations of the drill collars controlled by the common PI.

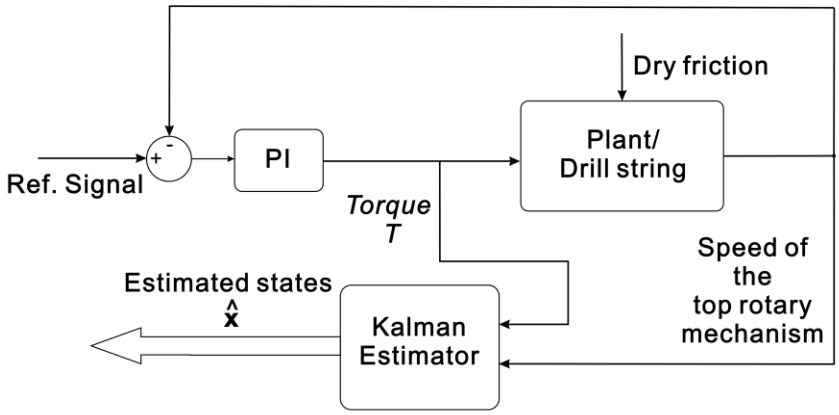


Fig.10. Schematic of a drill string with PI controller and Kalman estimator.

For the Kalman estimator design, the weighing factors $Q$ and $\mathbf{R}$ respectively represent the confidence on the measurement and the model. The selection of a large $Q$ would compel the estimator to rely more on the measurement signal. On the other hand, large $\mathbf{R}$ reduces the observer gain, which may result in a failure to update the propagated disturbance term based on the measurement (Girsang and Dhupia, 2013 and George et al., 2008). In this study, the weighting factor $Q$ = 35 and weight matrix $\mathbf{R} = \begin{bmatrix} 10^{-5} & 0 \\ 0 & 10^{-5} \end{bmatrix}$ were chosen to calculate the Kalman gain $\mathbf{L}$.

To validate the effectiveness of Kalman estimator in identifying the occurrence of stick-slip vibration (under the conditions as shown in Fig. 7), the true plant model described in Eqs. (2) – (16) along with the tuned PI controller is augmented with the Kalman estimator, as shown in Fig. 10. The inputs to the estimator are the controlled input torque $T$ and measurements from the true plant $\phi_r$ and $\dot{\phi}_r$, which are available from measurements at the top rotary mechanism. Figure 11 compares the estimated and measured rotational speed of the drill bit. It can be seen that the proposed linear Kalman estimator is able to reflect the occurrence of the downhole stick-slip vibration. It also provides a good estimate of the amplitude of the bit speed, which is critical to assess the severity of the vibrations. However, the estimation errors are significantly larger when the drill bit is in the stick region. As illustrated in Fig. 12, this phenomenon is because the linear estimator cannot estimate the nonlinear pre-sliding phase nor the sudden changes in friction torques with respect to rotational speed due to the hysteretic effect.

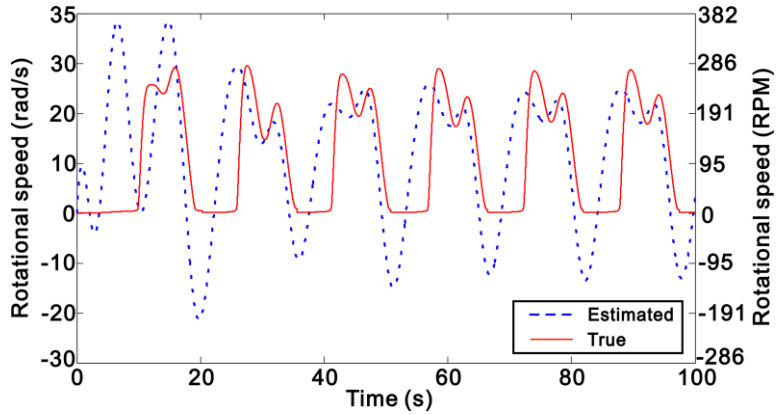


Fig. 11. Estimated and "true" rotational speeds during stick-slip vibrations.

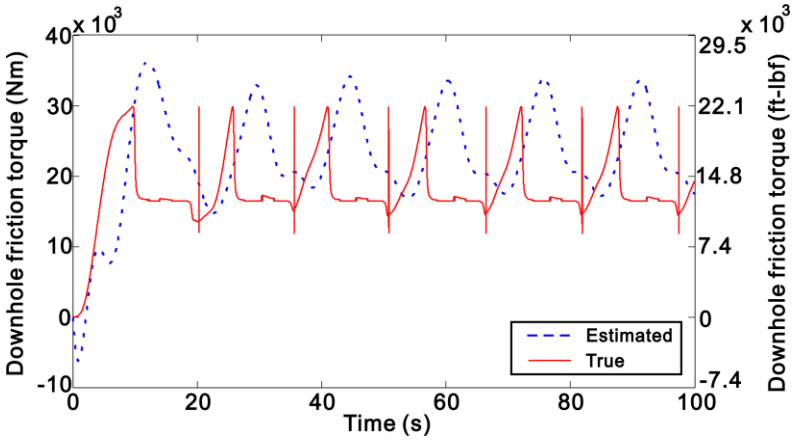


Fig. 12. Estimated and "true" downhole friction torque during stick-slip vibrations.

To calculate the controller gains **K**, the tuned weighting matrix $\mathbf{Q}_c = \begin{bmatrix} 200 & 0 & 0 & 0 \\ 0 & 200 & 0 & 0 \\ 0 & 0 & 300 & 0 \\ 0 & 0 & 0 & 300 \end{bmatrix}$ and the weighting factor $R_c$ = 0.01 were used. Here, the weighting matrix $\mathbf{Q}_c$ was chosen to reflect the relative importance of each state, putting more emphasis on controlling the speed rather than the position, while the weighting factor $R_c$ is to adjust how rigorous the control effort is. The resulting gains are

$$\mathbf{K} = \begin{bmatrix} 212.3 & -12.3 & 1141.5 & 196.9 \end{bmatrix} \tag{32}$$

Figure 13 shows the controlled response of the drill string using the proposed LQG control strategy (Fig. 5). The controller is able to suppress any excessive vibrations within 30 seconds from the start of simulation, by preventing the drill bit from falling

back to the stick region, after the drill bit remained stationary for the first 20 seconds. This performance is acceptable in common industrial practices (National Oilwell Varco, 2012; Lopez, 2009). As the top rotatory mechanism starts driving, the drill bit is still nearly stationary because the frictional characteristic is in the nonlinear pre-sliding region. This nonlinear friction contributes to the significant errors in the estimated drill bit speed, as shown in Fig. 14. However, after the drill bit begins to slide, the state estimates the true values resulting in a satisfactory control performance. As shown in Fig. 13 and 14, the ability of the proposed LQG control strategy to estimate the friction characteristics and states in the sliding region allow for a reliable control performance despite keeping a linear control structure. The steady-state error between the estimated and true friction torque shown in Fig. 15 may arise due to the order reduction of the model and the nonlinearity of the downhole dry friction. Nonetheless, the estimated friction torque still provides valuable insights on the profile of the downhole friction

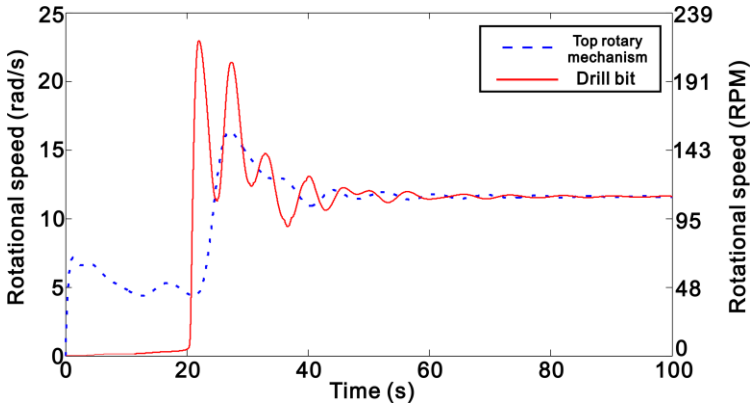


Fig. 13. Rotational speed of the top rotary mechanism on the surface and the drill bit in the downhole using the proposed control strategy.

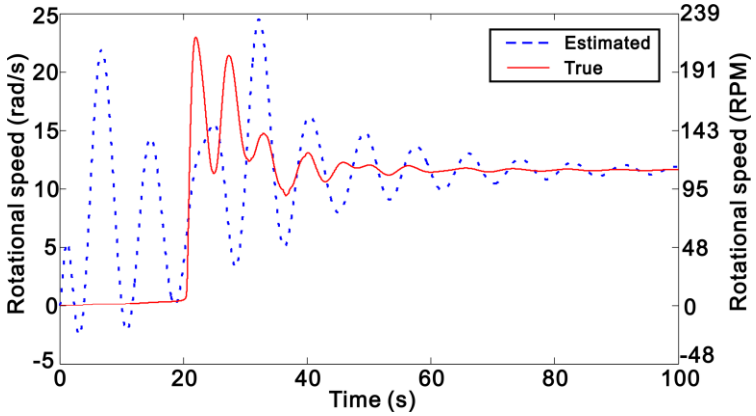


Fig. 14. Estimated and "true" rotational speeds of the drill bit during using the proposed control strategy.

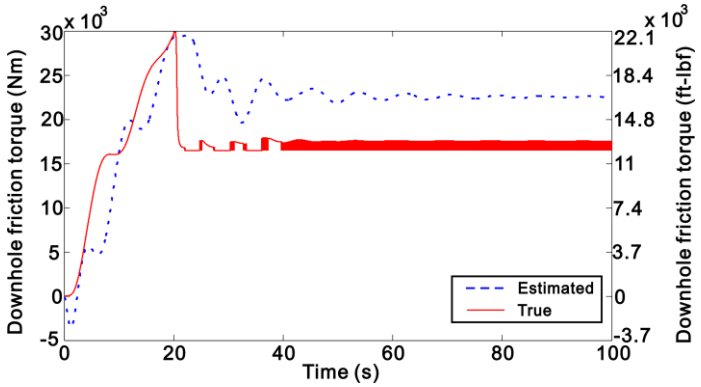


Fig. 15. Estimated and "true" downhole friction torque without stick-slip vibration when using proposed control strategy.

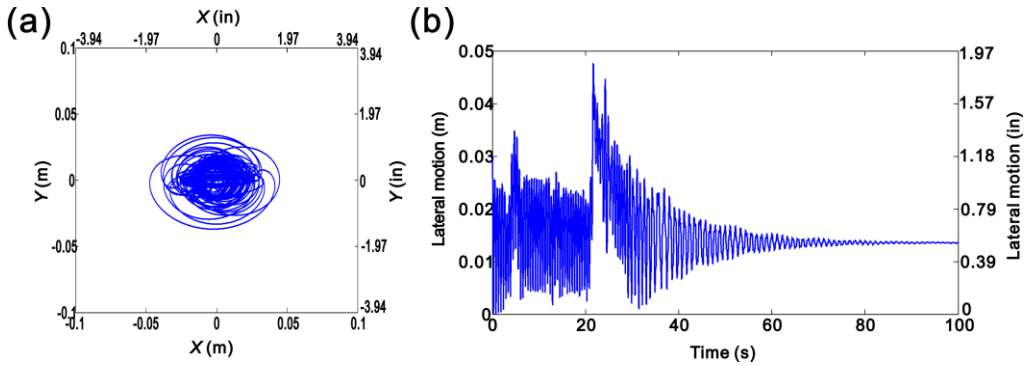


Fig. 16. (a) Trajectory of the geometric center of the drill collars controlled by the proposed controller with Kalman estimator; (b) Lateral vibrations of the drill collars controlled by the proposed controller with Kalman estimator.

without any downhole measurements. The lateral vibrations for this case are shown in Fig. 16, showing that the lateral motion is reduced to a steady-state whirling motion with small amplitudes after the transients. Therefore, even though the estimator model has not considered any lateral motions, the proposed control strategy is able to significantly mitigate the lateral vibrations and prevent the stick-slip response. Thus, the proposed LQG control strategy is successful in identifying of stick-slip vibrations, regulating the speed of the drill string and suppressing both torsional and lateral vibrations.

## 5. Conclusions

The excessive torsional and lateral vibrations of the BHA are usually the root causes for premature failures of the drill strings and low drilling efficiency. To mitigate these undesired vibrations in drill strings, state-space based controllers have been designed but

they usually require measurements from the downhole components, which are not easy to implement. To alleviate the requirements for downhole measurements, the use of Kalman estimator is proposed in this work to estimate the downhole states. This work includes a state for modeling the nonlinear downhole friction torque as a linear persistent disturbance. It has been shown that the designed estimator can effectively identify the occurrence of stick-slip vibration. Furthermore, an LQG strategy has been implemented on the estimated states to prevent the torsional stick-slip vibration and to mitigate the coupled lateral vibration of drill string. While the controller is designed using a reduced order two degree of freedom model, a high fidelity lumped parameter model of the drill string has been developed to validate the proposed control performance through numerical simulations. This extended model accounts for the coupled lateral motion of drill collars with the torsional motion of the rotational inertias of the top rotary mechanism, drill pipes, drill collar and drill bit. The downhole friction force has also been considered as a hysteretic dry friction model based on previous measurements from an experimental research rig. Simulation results indicate the effectiveness of the proposed LQG control scheme in estimating downhole states, mitigating stick-slip vibrations and regulating the drill bit velocity.

**Acknowledgements**

We are pleased to acknowledge the financial support (grant: M4061316) of Maritime Port Authority of Singapore and ABB Pte. (Singapore) Ltd. We are also grateful for several discussions with Mr. Louis Kennedy, Dr. Alf Kare Adnanes and Dr. Tegoeh Tjahjowidodo on the process models for drilling rig systems and the mitigation of the stick-slip vibrations.

**Appendix**

The system parameters used in simulation are

$J_r$ = 930 kgm$^2$ = 2.2×10$^4$ lb-ft$^2$; $J_p$ = 2122 kgm$^2$ = 5×10$^4$ lb-ft$^2$; $J_c$ = 549 kgm$^2$ = 1.3×10$^4$ lb-ft$^2$; $m$= 3941 kg = 8688 lb; $J_b$ = 370 kgm$^2$ = 8700 lb-ft$^2$; $k_p$= 700 Nm/rad = 516 ft-lb/rad; $k_c$ = 1080 Nm/rad = 797 ft-lb/rad; $k_b$ = 907 Nm/rad = 669 ft-lb/rad; $k$ = 1.4×10$^5$ N/m = 799 lbf/in; $k_w$= 1×10$^8$ N/m = 5.7×10$^5$ lbf/in; $c_r$ = 425 Nms/rad = 313 ft-lb-s/rad; $c_p$

= 140 Nms/rad = 103 ft-lb-s/rad; $c_c$ = 190 Nms/rad = 140 ft-lb-s/rad; $c_b$ = 181 Nms/rad = 133 ft-lb-s/rad; $c_m$ = 50 Nms/rad = 37 ft-lb-s/rad; $c$ = 387 Ns/m = 2.2 lb-s/in; $c_w$ = 437 Ns/m = 2.7 lb-s/in; $R$ = 0.1143 m = 4.5 in; $R_h$= 0.2143 m = 8.4 in; $e_0$=0.01 m = 0.4 in; WOB = $3\times10^5$ N = $6.7\times10^4$ lbf; $u_w$=0.05.

**References**


Jansen, J. D. and Steen, L. van den, 1995. Active damping of self-excited torsional vibrations in oil well drillstring. J. Vib. Acoust. 179, 647-668.

Leine, R. I., Campen, D. H. van and Keultjes, W. J. G, 2002. Stick-slip whirl interaction in drillstring dynamics. J. Sound Vib. 124, 209-220.

Tjahjowidodo, T., (2012). Theoretical analysis of the dynamic behavior of presliding rolling friction, Mech. Sys. Signal Proc. 29, 296-309.

National Oilwell Varco, 2012. Softspeed control loop with ABB gateway controllers.

Yigit, A. S. and Christoforou, A. P., 1998. Coupled torsional and bending vibrations of drillstrings subject to impact with friction. J. Sound Vib. 215, 167-181.

Al-Hiddabi, S. A., Samanta, B. and Seibi, A., 2003. Non-linear control of torsional and bending vibrations of oilwell drillstrings. J. Sound Vib. 265, 401-415.

Zamanian, M., Khadem, S. E. and Ghazavi, M. R., 2007. Stick-slip oscillations of drag bits by considering damping of drilling mud and active damping system. J. Petroleum Sci. Eng. 59, 289-299.

Richard, T., Germay C. and Detournay E., 2007. A simplified model to explore the root cause of stick-slip vibrations in drilling systems with drag bits. J. Sound Vib. 305, 432-456.

Ritto, T. G., Soize, C. and Sampaio, 2009. Non-linear dynamics of a drill string with uncertain model of the bit-rock interaction. Inter. J. Non-linear Mechanics. 44, 865-876.

Yigit, A. S. and Chistoforou, A. P., 2002. Coupled torsional and bending vibrations of actively controlled drillstrings. J. Sound Vib. 234, 67-83.

Jansen, J. D., 1991. Non-linear rotor dynamics as applied to oilwell drillstring vibrations. J. Sound Vib. 147, 115-135.

Puebla, H. and Alvarez-Ramirez, J., 2008. Suppression of stick-slip in drillstrings: A control approach based on modeling error compensation. J. Sound Vib. 310, 881-901.

Navarro-Lopez, E. M. and Cortes, D. 2007a. Avoiding harmful oscillations in a drillstring through dynamical analysis. J. Sound Vib. 307, 152-171.

Navarro-Lopez, E. M. and Cortes, D. 2007b. Sliding-mode control of a multi-DOF oilwell drillstring with stick-slip oscillations. American Control Con.

Hong, L. and Dhupia, J. S., 2015. Modeling and control of coupled torsional and lateral vibrations in drill strings. ASME Dyna. System and Control Con. (submitted).

Girsang, I. P., Dhupia, J. S., Mujadi, E., Singh, M. and Pao, L. Y., Gearbox and drivetrain models to study dynamic effects of modern wind turbines. IEEE trans. Industry App. 50, 3777-3786.

Tucker, W. R. and Wang, C. 1999. An integrated model for drill string dynamics," Journal of Sound and Vibration. J. Sound Vib. 224, 123-165.

Jansen, J. D., 1993. Nonlinear dynamics of oilwell drillstrings. Ph.D. Thesis.

Wojewoda, J., Stefanski, A., Weiercigroch, M. and Kapitaniak T, 2008. Hysteretic effects of dry friction: modelling and experimental studies. Math. Phy. Eng. Sci. 366, 747-765.

Girsang, I. P. and Dhupia, J. S., 2013. Collective pitch control of wind turbines using stochastic disturbance accommodating control. Wind Eng. 37, 517-534.

George, J., Singla, P. and Crassidis, J. L., 2008. Stochastic disturbance accommodating control using a Kalman estimator. Proc. AIAA Guidance, Navigation and Control Con. and Ex.

Freudenberg, J. S., Hollot, C. V. and Looze, D. P, 2013. A first graduate course in feedback control.

Navarro-Lopez, E. M. and Suarez, R., 2004. Practical approach to modelling and controlling stick-slip oscillations in oilwell drillstrings. IEEE Inter. Con. on Control Application.

Navarro-Lopez, E. M. and Suarez, R., 2009. An alternative characterization of bit-sticking phenomena in a multi-degree-of-freedom controlled drillstring. Nonlinear Ana: Real World Applications. 10, 3162-3174.